Recent additions to the PROFUSION code for the spurious mode analysis of the ECRH launchers for ITER

Burkhard Plaum[1*]

[1]Institute of Interfacial Process Engineering and Plasma Technology, University of Stuttgart, D 70569 Stuttgart, Germany

Abstract. Several new features were added to the PROFUSION code package in order to accurately simulate the optical part of the upper launcher for the ECRH system for ITER. The most important addition was the implementation of a generic "Physical Optics Surface", which utilizes the surface equivalence principle in order to analyse the effect of non-planar apertures on the generation of stray power and the radiated beams.

1 Introduction

In high power millimetre wave transmission systems, even small unwanted effects can have an impact on the system functionality. Therefore, a precise knowledge of the fields and loss mechanisms for realistic scenarios is required during the design phase. An important issue is the effect of higher order modes (HOMs) on the performance of the equatorial and upper ECRH launchers for ITER. The exact simulation of mode mixtures in optical systems requires the knowledge of the complex mode amplitudes. These are, however, impossible to predict because HOMs are mostly the result of manufacturing tolerances or assembly errors. Furthermore, time dependent phenomena, like thermal expansion of waveguides or long-term movement of buildings, play a role. Therefore, a Monte Carlo approach is the only option to assess the robustness of a system with respect to different spectra of HOMs [1].

The most important parameters are the truncation losses due to finite mirror sizes and the opening in the blanket shield module (BSM). Since higher order waveguide modes have a larger beam divergence when radiating in free space, they strongly influence the truncation losses. The truncated power is reflected by the internal metallic structures of the launcher and will ultimately contribute to the stray radiation level. Other important parameters are the peak power loading on the mirrors and the beam sizes in the plasma.

In order to run the Monte Carlo Method with thousands of mode mixtures within a reasonable time, we use the superposition principle: The time-consuming solvers are run just with the pure waveguide modes at the input and the fields at the locations of interest (e.g. the mirror surfaces) are saved in terms of complex vectors. The actual analysis is then done on linear combinations of these fundamental solutions. This speeds up the analysis by several orders of magnitude.

2 Model of the launcher

The launcher is simulated with the PROFUSION code package [2]. The principle model is shown in Fig. 1. Each of the 8 beams is directed via 4 mirrors towards the opening in the blanket shield module (BSM). For the focusing mirrors M1 and M3 we use the ellipsoid parameters to generate the surface description. Furthermore, the boundaries of the mirrors and the BSM opening are given in terms of 3D polygons.

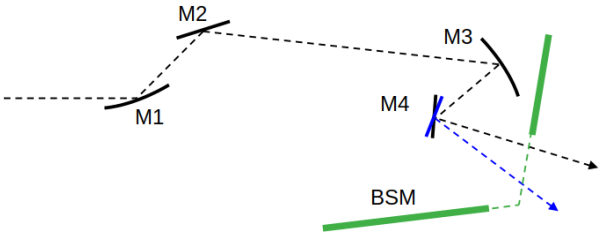

Fig. 1 Model of the upper launcher used for the simulation

The mirror reflection is calculated with a physical optics method, which was already used in other projects and benchmarked against the Zemax software and analytical methods [3].

Truncation effects can be simulated by calculating the field distribution on the surface (e.g. a mirror) and integrating the power inside of the boundary. By subtracting the integrated power of two consecutive mirrors, we get values for the truncation loss of each mirror.

To simulate the influence of the BSM opening on the radiated beam, however, a new solver was necessary, because the existing FFT based propagator in PROFUSION requires the initial field to be defined on a planar surface.

* Corresponding author: burkhard.plaum@igvp.uni-stuttgart.de

3 PO surface

To accurately simulate the influence of the non-planar BSM opening on the beam launched into the plasma, we utilize the surface equivalence principle (see Fig. 2): If we have a closed volume with arbitrary electromagnetic sources inside, we can replace them by a distribution of electric and magnetic currents on the surface, such that the external fields E_o and H_o are the same.

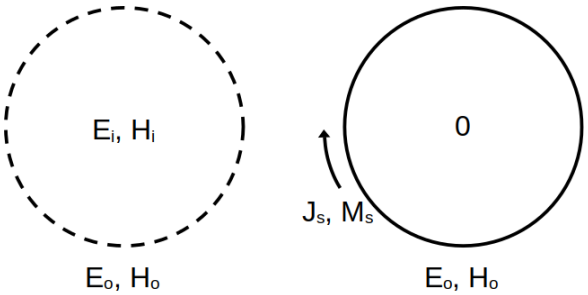

Fig. 2 Surface equivalence principle

This principle, which is a generalization of the Huygens principle, is used in many algorithms, such as the Boundary Element Method. In our application, however, we make some simplifications. Most notably, we assume a pure forward propagation (i.e. without reflections), such that the currents on the surface can be calculated simply from the incident fields.

This principle results in a solver, which is called "PO (Physical Optics) surface". It is outlined in Fig. 3. The surface can have an almost arbitrary shape, where the only limitation is, that there must be a direct line of sight from a field point to any point on the surface. Also, when the field is propagated from one surface to another one, the surfaces must not intersect. The surfaces are discretized into pixels, which have a size of about 0.25 λ. The incident fields E_i and H_i are calculated for each pixel. Together with the local normal vector, we then obtain the power density (for calculating the truncation loss).

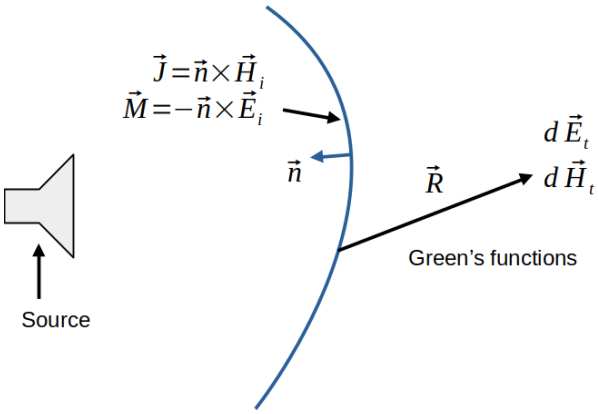

Fig. 3 Physical Optics (PO) surface

The transmitted fields E_t and H_t are then calculated with the Green's functions of radiating current elements in free space:

$$\vec{E}_t = -jk_0Z_0 \iint_S \left\{\left[1-\frac{j}{k_0R}-\frac{1}{(k_0R)^2}\right]\vec{J}(r') + \left[1-\frac{3j}{k_0R}-\frac{3}{(k_0R)^2}\right]\left(\hat{R}\cdot\vec{J}(r')\right)\hat{R}\right\}\frac{e^{-jk_0R}}{4\pi R}dS' + jk_0\iint_S \left[1-\frac{j}{k_0R}\right](\hat{R}\times\vec{M}(r'))\frac{e^{-jk_0R}}{4\pi R}dS' \quad (1)$$

$$\vec{H}_t = -jk_0Y_0 \iint_S \left\{\left[1-\frac{j}{k_0R}-\frac{1}{(k_0R)^2}\right]\vec{M}(r') + \left[1-\frac{3j}{k_0R}-\frac{3}{(k_0R)^2}\right]\left(\hat{R}\cdot\vec{M}(r')\right)\hat{R}\right\}\frac{e^{-jk_0R}}{4\pi R}dS' - jk_0\iint_S \left[1-\frac{j}{k_0R}\right](\hat{R}\times\vec{J}(r'))\frac{e^{-jk_0R}}{4\pi R}dS' \quad (2)$$

where $\vec{R}$ is the vector from the surface element to the field location and $\hat{R}=\vec{R}/R$. These versions of the Green's functions also contain the near field terms to ensure the maximum possible accuracy.

The PO surface is a generalization of the solver for metallic reflectors, which was integrated into the new framework. In addition, there are now frontends for:

- The illumination of a PO surface by a PROFUSION field source
- The propagation from one PO surface to another one
- The calculation of the radiated field, either in a plane or at single points
- The analysis of the field distribution on the surface for deriving truncation losses and peak power densities

An important addition was to have all these operation in separate executables, such that the analysis can also be done on linear combinations of mirror fields.

To benchmark the new code, a simple field propagation from an open ended HE11 waveguide was calculated and compared against the old FFT based propagator. At the distance of 585.2 mm, near field effects are still dominant. The results are shown in Fig. *4*. The agreement is very good. Some artefacts are visible in the FFT result. They are interferences from the virtual neighbour beams, which are always present in FFT based methods. The PO surface does not suffer from these problems and can therefore be considered the more accurate of both methods.

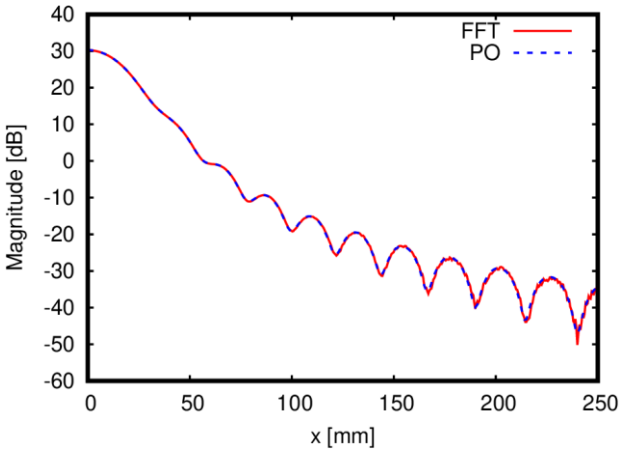

Fig. 4. Radiated field of a 50 mm HE11 waveguide (170 GHz) at a distance of 585.2 mm

4 Generation of the surface from the contour

The code for the representation of a discretized non-planar surface was taken from the existing mirror solver. The surface is implemented as a height map in cartesian coordinates, where x and y are on a regular grid with constant step sizes Δx and Δy and one z coordinate is assigned to each point. If such a surface is to be generated from a contour line (given as a closed 3D polygon) there is an infinite number of possible solutions.

Our approach uses the contour line and one additional "centre point", which is supposed to be on the surface as well. From this centre point, we make lines to each of the points on the boundary, resulting in a series of triangles. On each of these triangles, we can calculate the z-values by a simple interpolation using barycentric coordinates. This results in a straightforward method to synthesize a surface from a given boundary curve. The results for the BSM opening can be seen in Fig. 5.
A possible future extension could be a more general definition of a surface in terms of a triangle mesh.

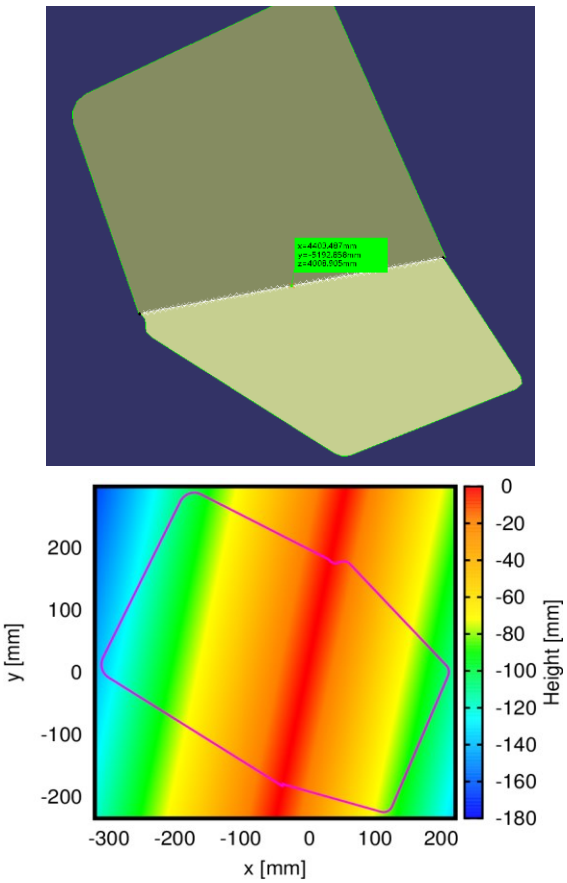

Fig. 5 Contour of the BSM opening with the center point (top) and the resulting height map (bottom)

5 Field distributions

The fields of the first beam (U1) in the BSM opening are shown in Fig. 6. We can see how the pattern moves according to the steering position. The fields of the U1 beam at a distance of 2 m from M4 are shown in Fig. 7 for 3 steering positions.

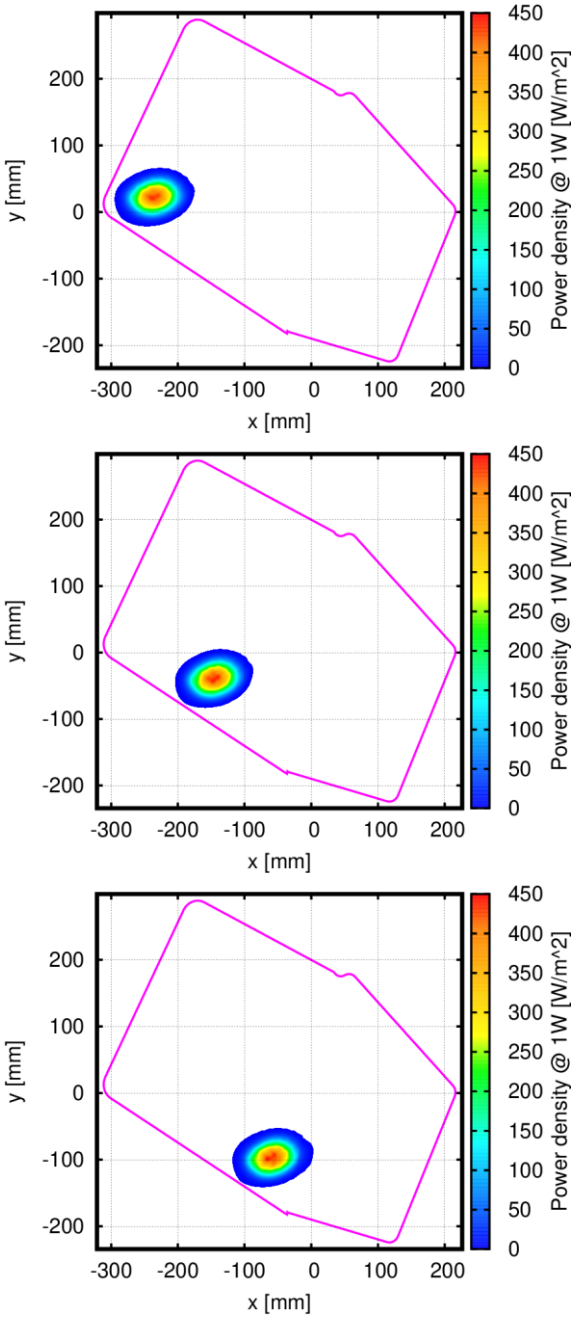

Fig. 6 Fields in the BSM opening for a steering angle of -6.5° (top), 0° (middle) and 6.5° (bottom)

The patterns look identical as expected for a planar steering mirror. The coordinate systems of the plots in Fig. 7 are centred around the beam axes for the 3 steering positions, which were obtained from ITER. The field maxima of the calculated beams are positioned exactly on the centres of the coordinate systems, which is another indication for the correctness of the model and the involved solvers. The exact centres of the corresponding fundamental Gaussian Beams were obtained with a fitting algorithm and the maximum deviation from the reference positions was 43µm.

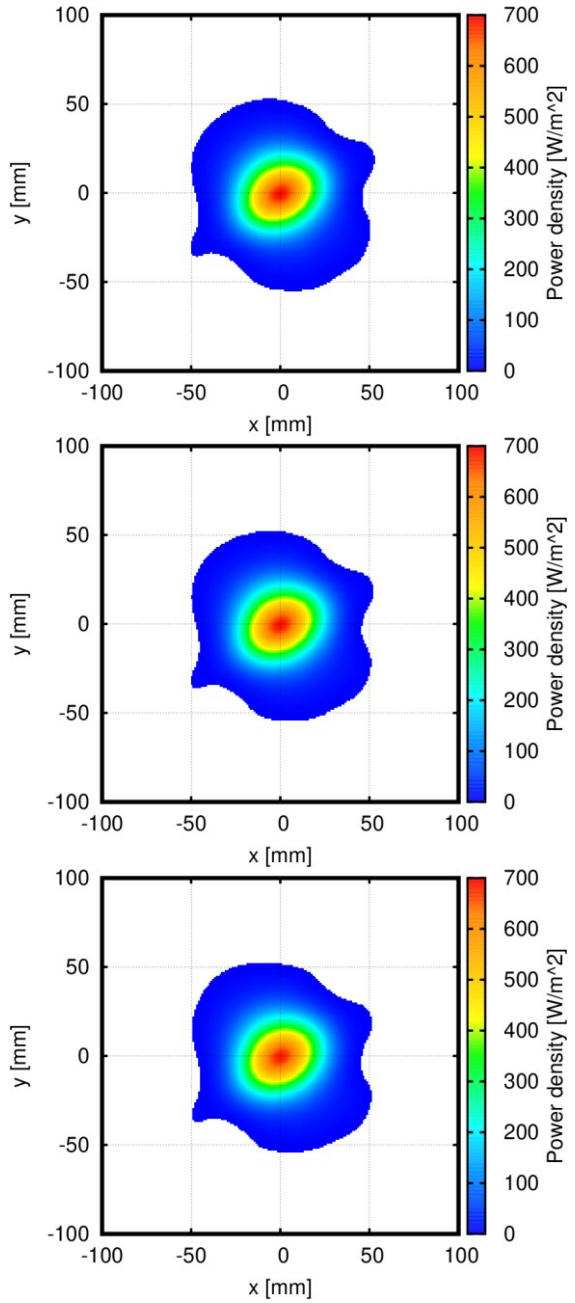

Fig. 7 Fields 2 m after M4 for a steering angle of -6.5° (top), 0° (middle) and 6.5° (bottom)

6 Truncation losses

The calculated truncation losses for the U-beams are shown in Table 1. They are similar to earlier results obtained by GRASP. A detailed comparison with more recent GRASP calculations [4] will be done in the near future.

Table 1. Calculated truncation losses

Location		U1	U2	U3	U4
M1		0.259	0.315	0.314	0.251
M2		0.261	0.281	0.284	0.255
M3		0.093	0.076	0.114	0.351
M4	**-6.5°**	0.168	0.037	0.036	0.323
	0.0°	0.227	0.069	0.061	0.375
	6.5°	0.375	0.143	0.121	0.484
BSM	**-6.5°**	0.028	0.003	0.004	0.032
	0.0°	0.037	0.002	0.001	0.018
	6.5°	0.050	0.003	0.002	0.027

7 Conclusion and Outlook

The PO surface was a major addition to the PROFUSION code package, which enables the calculation of several new classes of problems. For the current projects, it can be used to simulate the effects of almost arbitrary obstacles in the beam path, which can be described in terms of a 3D boundary curve.

In the future, the PO surface can be extended to represent the interface between two dielectric media with different refractive indices. This would enable the simulation of windows and lenses. In these cases, however, we need an iterative procedure in order to track the multiple internal reflections until we obtain a stationary result.

References

1. B. Plaum, Estimation of the Effects of Spurious Modes in Linear Microwave Systems Using a Monte Carlo Algorithm. IEEE Journal of Microwaves **3**, 1061-1067 (2023). https://doi.org/10.1109/JMW.2023.3283152
2. B. Plaum, Simulation of microwave beams with PROFUSION (2022 Edition). http://elib.uni-stuttgart.de/handle/11682/12258.
3. B. Plaum, M. Preynas and M. Choe, Calculations for the optical system for the first ITER plasma. EPJ Web Conf., **277**, 01005 **(**2023). https://doi.org/10.1051/epjconf/202327701005
4. P. Platania, A. Simonetto et.al., Electromagnetic Simulations of the ITER Upper Launcher, *this conference*